Enhanced lens by ϵ and μ near-zero metamaterial boosted by extraordinary optical transmission

Miguel Navarro-Cía,[1] Miguel Beruete,[1] Igor Campillo,[2] and Mario Sorolla[1]

[1]*Millimeter and Terahertz Waves Laboratory, Universidad Pública de Navarra, Campus Arrosadía, E-31006 Pamplona, Spain*
[2]*CIC nanoGUNE Consolider, Tolosa Hiribidea 76, E-20018 Donostia, Spain*
(Received 2 December 2010; published 7 March 2011)

In this paper we report directivity enhancement by a short-focal-length plano-concave lens engineered by stacked subwavelength hole arrays (fishnet-like stack) with an effective negative index of refraction close to zero, $n \to 0$, that arises from ε and μ near-zero extreme values. The plano-concave lens frequency response shows two enhancement peaks, one at the wavelength corresponding to $n = -1$ and, prominent in this configuration, another unexpected peak when $n \to 0$ that comes as a result of the similar low values of ε and μ. The frequency-dependent negative refractive index and beam-forming properties of the lens are supported by finite-integration-frequency- and time-domain simulations and experimental results. This near-zero metamaterial lens can find applications in terahertz and even optics since the building block, stacked extraordinary optical transmission layers, has already been reported for those regimes under the name of fishnet structure.

I. INTRODUCTION

The growth in metamaterials research and development has largely been driven by the ability to extend the range of a material's electromagnetic properties by using artificial media with effective indices of refraction close to −1, which are a particular case of the so-called negative index media (NIM).[1,2] In this framework, several lenses based on split-ring resonators[3] or even photonic crystals[4,5] have been reported with plano-concave profiles. Recently, extreme-parameter metamaterials (ε or μ near zero) have even attracted more attention in metamaterials research,[6–11] showing that the discoveries in this field seem to be limitless. At such extremely low values in the vicinity of the plasma frequency, there are no sharp resonances in the Drude-Lorentz model, and therefore, according to Kramers-Krönig relations, fewer ohmic losses than near resonance frequencies (where classical resonance-based NIM are designed) are expected.[12] The attempts to implement them as wave-front converters have been limited to numerical calculations[9–11] and a few experiments in electromagnetic bandgap (EBG) structures at microwaves,[8,13] despite their potential.

Stimulated by the breakthroughs of metamaterials at microwaves, researchers have been attempting to come up with a low-loss metamaterial that allows tailoring the electric permittivity ε and the magnetic permeability μ for impedance matching suitable for high frequencies. Among other resonance-based approaches, where the negative index of refraction is achieved via resonant response in ε (usually exploiting Drude dispersion) and μ (Lorentz-like dispersion), fishnet structures[14,15] have the best performance. However, losses can be further minimized by designing those fishnet layers under extraordinary optical transmission (EOT) criteria,[16] as was reported for millimeter waves.[17,18] Encouraged by the success of the extraordinary optical transmission metamaterial (EOTM) and its effective negative index of refraction, which was confirmed by wedge experiments at different wavelengths,[19–22] we embarked on the pursuit of beam-forming applications based on EOTM technology.[23–28]

Here we extend our previous work of plano- and bi-concave metamaterial lenses exhibiting an index of refraction $n_z = -1$

(Refs. 23–28) by studying the response of the EOTM lens when the effective negative index of refraction approaches zero. In Ref. 25 we already highlighted the high enhancement measured at 5.24 mm (57.2 GHz), when $n_z \sim 0$, for a biconcave configuration, but this enhancement was not further analyzed. Now, we use this feature to transform an isotropic source into a plane-wave-like beam at the millimeter-wave range.[8–11] One of the main advantages of NZM lenses is that ohmic losses are expected to be negligible because we are far from the resonant frequencies of the Drude and Lorentz responses of the electric permittivity and magnetic permeability, respectively. Moreover, given its ability to tailor both ε and μ, the NZM lens can potentially be free-space matched, unlike dielectric lenses.

II. DESIGN PARAMETERS AND APPROXIMATIONS

Details of the proposed EOTM lens, whose maximum side is 23.9 times the operation wavelength, can be found in Fig. 1 and in Refs. 24–28. In short, the unit cell parameters are as follows: in-plane period $d_x = 3$ mm and $d_y = 5$ mm, stack periodicity $d_z = 1.5$ mm, hole diameter $a = 2.5$ mm, and metal thickness $t = 0.5$ mm. Different from previous works,[8,10,11,13] our lens falls within the realm of effective medium approximation (yet close to the EBG regime) since the stack periodicity is $d_z \approx 0.3\lambda$ and is all metallic. The curved face is approximated by a staircase profile with a step equal to the size of the cross-section dimensions of the unit cell of the EOTM. The plano-concave EOTM lens comprises 17 stacked layers. (The thinnest part of the EOTM lens is composed of two layers.)

In the incidence of an electromagnetic wave into a medium with an effective index of refraction near zero (without loss of generality, the first medium is air, $n_{air} = 1$), Snell's law imposes the restriction of angles of incidence close to $0°$ in order to have transmission. Thus, the ideal profile in this case would be a hemispherical shell.[29,30] Note that according to Fermat's principle and the related concept of optical path, a lens whose index of refraction is lower than the surrounding medium ($n_{lens} < n_{medium}$ and considering also negative values)
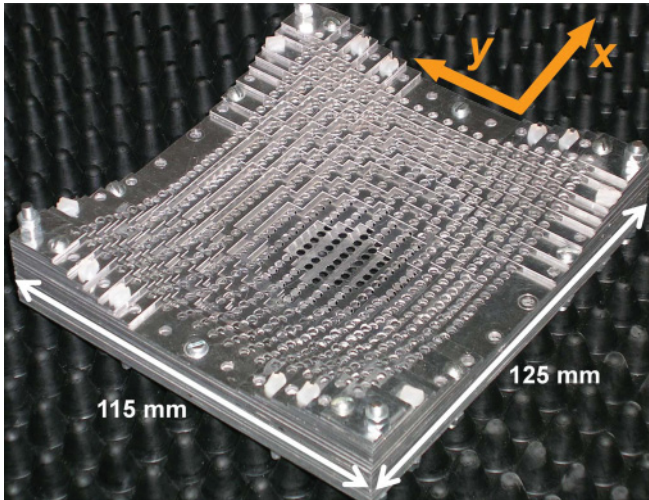
FIG. 1. (Color online) Picture of the fabricated prototype. The parameters of the unit cell are $d_x = 3$ mm, $d_y = 5$ mm, $d_z = 1.5$ mm ($\sim0.3\lambda$), hole diameter $a = 2.5$ mm, and metal thickness $t = 0.5$ mm.

FIG. 2. (Color online) (left) Sketch of the experimental setup and (right) detail of the illumination section. The dashed green lines depict the plane measured. Note that the set feeder and EOTM lens are placed over a rotary platform, which has been symbolized in the sketch by the green arrows.

must have a concave profile in order to transform a spherical wave front to a plane wave and vice versa.[29,30] This case is different from the ε-near-zero materials, where any arbitrary shape can be used at the input to obtain a plane wave at the output as long as polarization is TM and the output face is plane.[9] However, considering that our lens has a small numerical aperture, its parabolic profile can approximate reasonably well the ideal one. (Indeed, any lens profile at small angles is approximately the same as a hemispherical shell.[30])

III. EXPERIMENTAL RESULTS AND RETRIEVED EFFECTIVE PARAMETERS FROM S COEFFICIENTS

The ability of the lens to improve the transmitted power in the normal direction due to a collimation effect (equivalent to an enhancement of directivity in the far field) of an isotropic source was checked using the following experimental setup: a rectangular waveguide (3.8 mm $\times$ 1.9 mm (WR-15), whose TE$_{10}$ cutoff frequency is 39.9 GHz) ending in a resonant slot was used as an approximation to an ideal isotropic source with vertical polarization (electric field along the vertical dimension y) and was located at the experimental focal length $z = 45$ mm (Refs. 24–28) from the EOTM lens. The set feeder and EOTM lens were placed on a rotary platform to measure the angular beam pattern. On the other extreme, the output power was detected with a corrugated horn antenna fixed at 1900 mm from the sample; see Fig. 2. Both transmitter and receiver antennas were connected to the AB-Millimetre^{TM} Quasioptical Vector Network Analyzer, and the reference measurement (calibration procedure) was performed by putting antennas face to face without the EOTM lens in free space.

Figure 3 renders the angular distribution of the radiated beam in the H-cutting (xz) plane. A clear directivity enhancement (note that we are directly correlating the narrowing of the main lobe on one plane to an enhancement of the directivity, which, indeed, accounts for both planes) is recorded at $\lambda = 5.24$ mm (57.2 GHz). There is no other evidence of enhancement in the range between 5.12 and 5.30 mm [Fig. 3(a)]. The
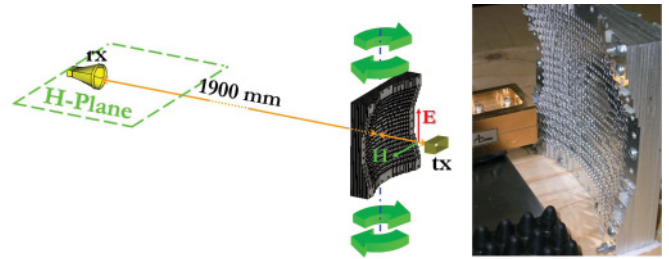
cross-polar measurement (receiving antenna rotated 90° with respect to the incident vertical electric field) remains very low with respect to the copolar measurement [Fig. 3(b)]. The origin of the cross-polar measurement may come from the modal nature supported by the circular hole since the fundamental mode (in cutoff because of the subwavelength dimensions) is the TE$_{11}$ (Ref. 31), which displays some x component. Therefore, a rectangular hole should reduce cross polarization because the fundamental mode is a TE$_{10}$ without x component.

From Fig. 3(a) the maximum transmittance (main lobe) of the copolar component reaches a value of 27 dB (in linear scale, a factor of 500 times), improving previous experimental results on EBGs.[8,13] Note that this happens at $+5°$ rather than at the optical axis [see Fig. 3(c)], where the value is 22 dB (a factor of 158), while the cross-polar measurement is 14 dB at $+5°$ and has a maximum value of 18.5 dB at $+10°$ [see Figs. 3(b) and 3(c)]. The slight displacement with respect to the optical axis may be due to an experimental misalignment.

The directivity enhancement at 5.24 mm is due to a refractive index approaching zero along with impedance matching, as demonstrated in Fig. 4. We have retrieved the constitutive parameters from the S-parameter simulation of two stacked layers (assuming small numerical aperture, the analysis of the lens can be reduced to its central zone) under normal incidence;[32–34] see Fig. 4. As we are working at angles close to normal, this analysis can be considered a reasonable, yet evident, simplification because anisotropy[35,36] is disregarded. (The importance of anisotropy in the response will be shown in the next section.) Note that the values shown in Fig. 4 are just a mathematical interpretation. They model the response of the mesoscopic stack for a certain set of conditions, and its extension to truly effective values somehow lacks physics.[12,34,37] For this numerical analysis, the electric conductivity of the aluminum was fixed to 3.72×10^7 S/m, and the problem was reduced to the unit cell with transversal periodic boundary conditions and solved with the frequency domain solver of CST Microwave Studio^{TM}.[38]

At $\lambda = 5.2$ mm (57.7 GHz), the calculation gives $\varepsilon = \mu = 0.37$ [Figs. 4(c) and 4(d)], with negligible imaginary parts. The consequences are twofold: first, the retrieved effective index of refraction is $n_z = 0.37$ with a negligible imaginary part [Fig. 4(b)]; second, the real outstanding feature is that the medium is perfectly matched with free space $\eta_{EOTM} = (\mu/\varepsilon)^{1/2} = 1$ [see Fig. 4(a)], which is the main advantage

(a)

(b)

(c)
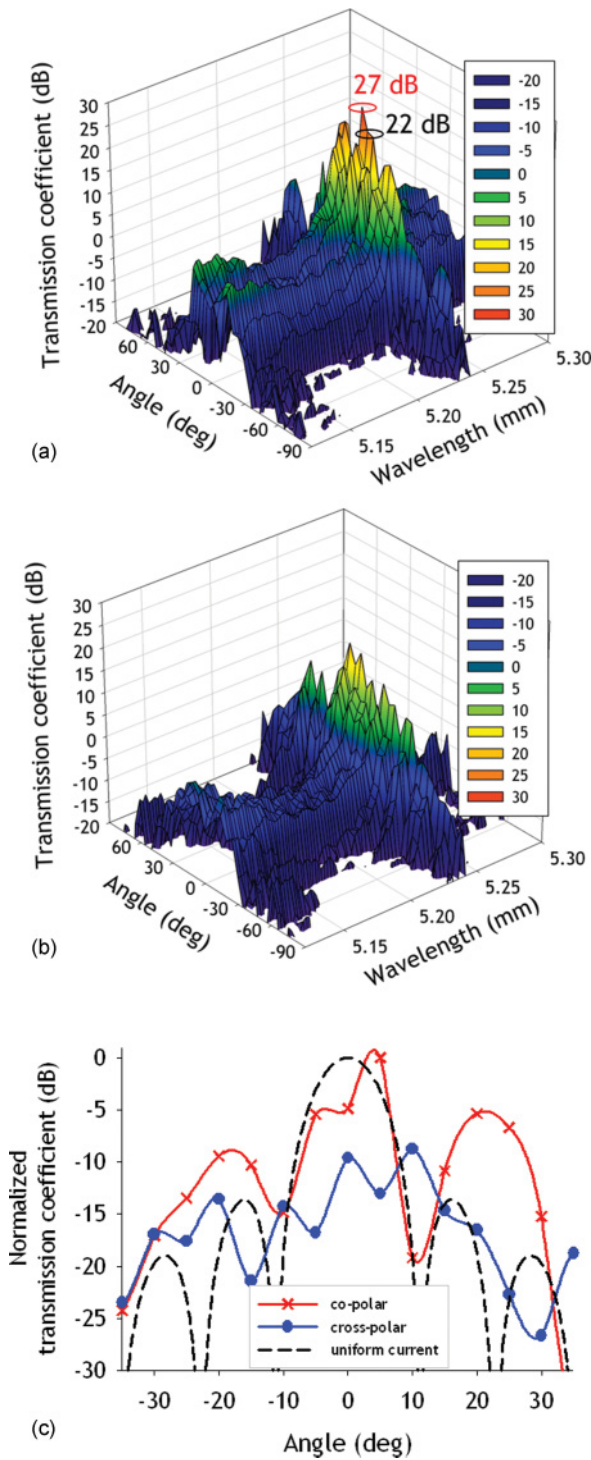
FIG. 3. (Color online) (a) Copolar and (b) cross-polar measurements of the angular power distribution as a function of frequency for the H plane. (c) Copolar (red crosses) and cross-polar (blue circles) measurements for the wavelength of maximum enhancement. The normalized power pattern of an x-directed uniform line source with the same dimensions as the central part of our lens (i.e., 9 holes $\times$ $d_x = 27$ mm) is shown as a dashed curve.

over metamaterials where ε or μ is near zero, which exhibit large difficulties in coupling the electromagnetic wave into them. Therefore, the EOTM lens is operating at 5.2 mm as a near-zero metamaterial (NZM) with small ohmic losses
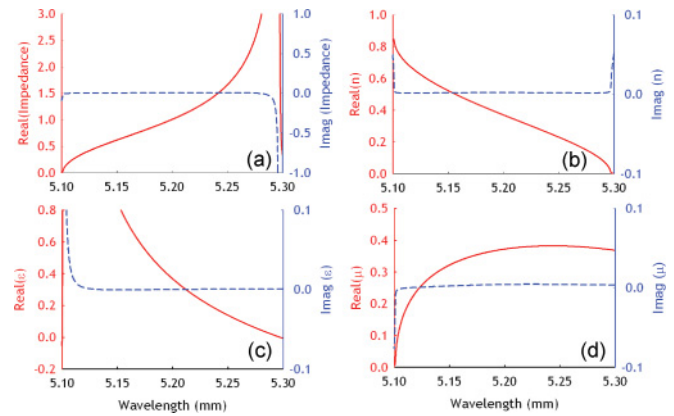
FIG. 4. (Color online) Retrieved constitutive parameters of the two-layer EOTM under normal incidence from numerical results. Real (red solid curve) and imaginary (blue dashed curve) parts of (a) normalized characteristic impedance, (b) effective index of refraction, (c) electric permittivity ε, and(d) magnetic permeability μ.

(small imaginary part) and is matched to free space. As an additional argument, it is well known that a uniform current leads to the radiation pattern with the highest directivity.[39] Assuming an ideal uniform current sheet source along x with the same dimensions as the central part of our lens (composed of two stacked layers) (i.e., 9 holes $\times$ $d_x = 27$ mm), the beamwidth between first nulls computed analytically leads to a value of 22.4°, similar to the measured values for the EOTM lens reported here: 21.4°. This suggests a true NZM performance since a perfect NZM would generate a uniform current at the output face.

The strongly selective behavior around the working frequency is also remarkable. At $\lambda = 5.24$ mm a maximum is observed in the experiment, whereas near this maximum a relative minimum appears at $\lambda = 5.18$ mm. This aspect is discussed in the next section.

IV. FINITE-INTEGRATION TIME-DOMAIN SIMULATIONS

In the preceding analysis, we supported our experimental results by simplifying the problem to two stacked layers and geometrical optics (Snell's law). However, the electromagnetic response of the EOTM lens is more complex since we are illuminating it in the near field: the focal length is 45 mm (8.6λ), whereas the far-field distance is $z_{\rm ff} = 2D^2/\lambda \approx 5960$ mm, where D is the diameter of the aperture.[39] To get a better approximation to the problem, the structure is now numerically analyzed with the time-domain solver of CST Microwave Studio.[38]

To gain more insight, we simulated the three-dimensional (3D) structure excited by a dipole at the focal length and recorded the field at 1900 mm (optical axis) with a far-field probe. In addition, the inverse problem was simulated (excitation by a plane wave from the flat face and detection by an open-ended waveguide at the focal length) so as to evaluate the importance of the receiver/feeder. Figure 5 shows the normalized transmission coefficient as a function of frequency for both scenarios. It is significant that both cases give rise to
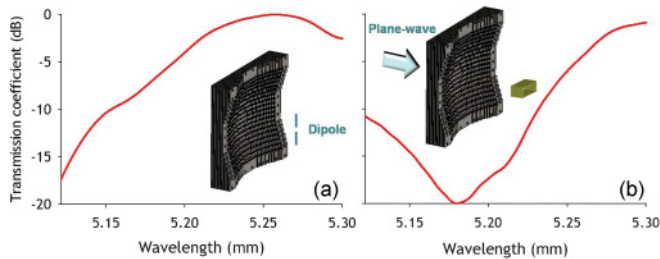
FIG. 5. (Color online) Simulated normalized transmitted power in logarithmic scale when the 3D EOTM lens is illuminated by (a) a dipole at the focal length with the field recorded by a far-field probe at 1900 mm and (b) a plane wave from its flat face with the receiving antenna located at the focal length is an open-ended waveguide.

a sudden decrease of the transmitted power in a narrow band (15 dB within a 0.13-mm span and 20 dB within a 0.12-mm span for each case), which is in qualitatively good agreement with the measured response.

An explanation can be found in the anisotropy of the structure. In the *H* plane the incident polarization is TE (or *S* polarization), and it has been demonstrated that in this case the numerical aperture is relatively high[35] and therefore that the field distribution should be similar for two close wavelengths. However, the story is fairly singular for the *E* plane. In this case, the TM (or *P*) polarization is relevant, and as discussed in Refs. 35 and 36, EOTM displays an extremely narrow numerical aperture. This means that in this *E* plane, we may have high frequency selectivity, which allows for a good transmission level at a particular wavelength like 5.24 mm but

a relatively low level at any other wavelength close to it such as 5.2 mm, which is what occurs in the experiment.

V. CONCLUSIONS

In conclusion, we have presented in this paper pencil-like radiation achieved by using a near-zero effective index of refraction metamaterial lens based on stacked extraordinary optical transmission layers at millimeter waves with high gain. In addition, cross-polar values remain low, which is an important feature from the technological perspective. These results along with the already-reported directivity enhancement of the EOTM lens at the frequency where the effective index of refraction is $n_z = -1$ (Refs. 24–28) allow us to consider the EOTM lens as a dual-band plane-wave-like beam-forming device. Moreover, an EBG behavior similar to that in Refs. 8, 10, 11, and 13 is likely to be attainable at higher frequencies (beyond the scope of this paper). Therefore, this EOTM lens could become a multifrequency device. Since the phenomenon of extraordinary transmission has been reported in all ranges of the spectrum, this technology has the possibility of being extended to any wavelength.

[1] V. G. Veselago, Sov. Phys. Usp. **10**, 509 (1968).

[2] J. B. Pendry, Phys. Rev. Lett. **85**, 3966 (2000).

[3] C. G. Parazzolli, R. B. Greegor, and M. H. Tanielian, in *Physics of Negative Refraction and Negative Index Materials*, edited by C. M. Krowne and Y. Zhang (Springer, Berlin, 2007), p. 261.

[4] P. Vodo, P. V. Parimi, W. T. Lu, and S. Sridar, Appl. Phys. Lett. **86**, 201108 (2005).

[5] B. Gralak, S. Enoch, and G. Tayeb, J. Opt. Soc. Am. A **17**, 1012 (2000).

[6] M. G. Silveirinha and N. Engheta, Phys. Rev. Lett. **97**, 157403 (2006).

[7] A. Alù and N. Engheta, Phys. Rev. E **72**, 016623 (2005).

[8] S. Enoch, G. Tayeb, P. Sabouroux, N. Guérin, and P. Vincent, Phys. Rev. Lett. **89**, 213902 (2002).

[9] A. Alù, M. G. Silveirinha, A. Salandrino, and N. Engheta, Phys. Rev. B **75**, 155410 (2007).

[10] R. W. Ziolkowski, Phys. Rev. E **70**, 046608 (2004).

[11] S. J. Franson and R. W. Ziolkowski, IEEE Antennas Wireless Propag. Lett. **8**, 387 (2009).

[12] L. Landau and E. M. Lifschitz, *Electrodynamics of Continuous Media* (Elsevier, New York, 1984).

[13] A. Martínez, M. A. Piqueras, and J. Martí, Appl. Phys. Lett. **89**, 131111 (2006).

[14] S. Zhang, W. Fan, N.C. Panoiu, K. J. Malloy, R. M. Osgood, and S. R. J. Brueck, Phys. Rev. Lett. **95**, 137404 (2005).

[15] G. Dolling, C. Enkrich, M. Wegener, C. M. Soukoulis, and S. Linden, Science **312**, 892 (2006).

[16] T. W. Ebbesen, H. J. Lezec, H. Ghaemi, T. Thio, and P. A. Wolf, Nature (London) **391**, 667 (1998).

[17] M. Beruete, M. Sorolla, and I. Campillo, Opt. Express **14**, 5445 (2006).

[18] M. Beruete, M. Sorolla, M. Navarro-Cía, F. Falcone, I. Campillo, and V. Lomakin, Opt. Express **15**, 1107 (2007).

[19] M. Navarro-Cía, M. Beruete, M. Sorolla, and I. Campillo, Opt. Express **16**, 560 (2008).

[20] M. Beruete, M. Navarro-Cía, F. Falcone, I. Campillo, and M. Sorolla, J. Phys. D **42**, 165504 (2009).

[21] J. Valentine, S. Zhang, T. Zentgraf, E. Ulin-Avila, D. A. Genov, G. Bartal, and X. Zhang, Nature (London) **455**, 376 (2008).

[22] M. Beruete, M. Navarro-Cía, F. Falcone, I. Campillo, and M. Sorolla, Opt. Lett. **35**, 643 (2010).

[23] M. Beruete, I. Campillo, J. E. Rodríguez-Seco, E. Perea, M. Navarro-Cía, I. J. Núñez-Manrique, and M. Sorolla, IEEE Microwave Wireless Compon. Lett. **17**, 831 (2007).

[24]M. Beruete, M. Navarro-Cía, M. Sorolla, and I. Campillo, Opt. Express **16**, 9677 (2008).

[25]M. Navarro-Cía, M. Beruete, M. Sorolla, and I. Campillo, Appl. Phys. Lett. **94**, 144107 (2009).

[26]M. Navarro-Cía, M. Beruete, M. Sorolla, and I. Campillo, Phys. B **405**, 2950 (2010).

[27]M. Navarro-Cía, M. Beruete, I. Campillo, and M. Sorolla, Metamaterials **4**, 119 (2010).

[28]M. Navarro-Cía, M. Beruete, I. Campillo, and M. Sorolla, IEEE Trans. Antennas Propag. (to be published).

[29]S. Cornbleet, *Microwave Optics—The Optics of Microwave Antenna Design* (Academic, New York, 1976).

[30]L. Solymar, and E. Shamonina, *Waves in Metamaterials* (Oxford University Press, New York, 2009).

[31]M. Beruete, I. Campillo, M. Navarro-Cía, F. Falcone, and M. Sorolla Ayza, IEEE Trans. Antennas Propag. **55**, 1514 (2007).

[32]X. Chen, T. M. Grzegorczyk, B.-I. Wu, J. Pacheco Jr., and J.A. Kong, Phys. Rev. E **70**, 016608 (2004).

[33]D. R. Smith, D.C. Vier, T. Koschny, and C.M. Soukoulis, Phys. Rev. E **71**, 036617 (2005).

[34]S. A. Ramamrishna and T. M. Grzegorczyk, *Physics and Applications of Negative Refractive Index Material* (CRC Press, Boca Raton, FL, 2009).

[35]M. Beruete, M. Navarro-Cía, and M. Sorolla, New J. Phys. **12**, 063037-1 (2010).

[36]M. Beruete, M. Navarro-Cía, M. Sorolla, and I. Campillo, Phys. Rev. B **79**, 195107 (2009).

[37]P. A. Belov, E. A. Yankovskaya, I. V. Melchakova, and C. R. Simovski, Opt. Spectrosc. (USSR) **109**, 90 (2010).

[38][http://www.cst.com].

[39]C. A Balanis, *Antenna Theory Analysis and Design* (Wiley, New York, 1997).